E-ISSN : 2541-5794
P-ISSN : 2503-216X

Journal of Geoscience,
Engineering, Environment, and Technology
Vol 02 No 02 2017

# Review : Marine Seismic And Side-Scan Sonar Investigations For Seabed Identification With Sonar System

Muhammad Zainuddin Lubis[1,*], Kasih Anggraini[2], Husnul Kausarian[3], Sri Pujiyati[4]

[1] *Department of Informatics Engineering, Geomatics Engineering Batam Polytechnic, Batam Kepulauan Riau, 29461 Indonesia.*
[2] *Research Center for Oceanography LIPI, Jakarta, Indonesia.*
[3] *Department of Geological Engineering, Universitas Islam Riau, Jl. Kaharudin Nasution No. 113, Pekanbaru, Riau 28284, Indonesia.*
[4] *Department of Marine Science and Technology, Bogor Agricultural University Jln. Agatis, Kampus IPB Dramaga Bogor 16680 Indonesia.*

* Corresponding author : zainuddinlubis@polibatam.ac.id
Tel+6281342578087, Office : 778-469856 ext : 2510; fax: +62-778-463620
Received: Mar 31, 2017. Revised : May 20, 2017, Accepted: May 31, 2017, Published: 1 June 2017
DOI: 10.24273/jgeet.2017.2.2.253

**Abstract**

Marine seismic reflection data have been collected for decades and since the mid-to late- 1980s much of this data is positioned relatively accurately. Marine geophysical acquisition of data is a very expensive process with the rates regularly ship through dozens of thousands of euros per day. Acquisition of seismic profiles has the position is determined by a DGPS system and navigation is performed by Hypack and Maxview software that also gives all the offsets for the equipment employed in the survey. Examples of some projects will be described in terms of the project goals and the geophysical equipment selected for each survey and specific geophysical systems according to with the scope of work. For amplitude side scan sonar image, and in the multi-frequency system, color, becoming a significant properties of the sea floor, the effect of which is a bully needs to be fixed. The main confounding effect is due to absorption of water; geometric spread; shape beam sonar function (combined transmit-receive sonar beam intensity as a function of tilt angle obtained in this sonar reference frame); sonar vehicle roll; form and function of the seabed backscatter (proportion incident on the seabed backscattered signal to sonar as a function of the angle of incidence relative to the sea floor); and the slope of the seabed. The different angles of view are generated by the translation of the sonar, because of the discrete steps involved by the sequential pings, the angular sampling of the bottom.

**Keywords:** Marine Seismic, Marine geophysical, Side Scan Sonar (SSS), Seabed, Angels

## 1. Introduction

Marine exploration with acoustic system has any function for: marine seismic, marine fisheries, determine abundance of fish in marine fisheries (Lubis and Manik, 2017), Fish stock estimation echosounder instrument with hydroacoustic system (Lubis and Wenang, 2016), Echo Processing and Identifying Surface and Bottom Layer (Lubis et al., 2016). Marine seismic reflection data have been collected for decades and since the mid-to late-1980s much of this data is positioned relatively accurately. This older data provides a valuable archive, however, it is mainly stored on paper records that do not allow easy integration with other datasets. Marine geophysical acquisition of data is a very expensive process with the rates regularly ship through dozens of thousands of euros per day. In addition, the survey often remote sites and can cause huge overhead on the transit time. sub-bottom reflection data has been collected for the Decade but much older data is stored with paperrecords and not so Easy to integrate with modern bathymetric data at this time (Owen et al., 2015).

Seismic reflection surveys have been used to map the sub-surface since 1921 with marine reflection surveys coming to prominence in the 1950s when they were used to map bathymetry, seabed identification using multibeam and side scan sonar instrument (Manik et al., 2014), seabed identification using side scan sonar C MAX- CM2 in punggur sea with acoustic method (Lubis et al., 2017).

Sonar system used sound to detect or find objects that are specifically located in the sea. Multibeam Sonar is an acoustic instrument that has the ability to perform three-dimensional mapping of the ocean floor (Bartholoma, 2006). The water depth measurement using multibeam instrument are fast and has a high accuracy, where this can not be done by a single beam echosounder. In addition to the instrument's ability to perform basic scanningthe seawater with very high accuracy and coverage are also able to produce information in the form of backscatteringvalues which can be used to determine the distribution ofseafloor sediment type (Manik, 2011).

Modern seismic data (including multichannel seismics, 3D seismics and parametric techniques),

stored, processed and interpreted digitally, can provide more detail than older data (Mohammedyasin et al., 2016). In particular, accurate analysis of reflector polarity (Yoo et al., 2013) may not be possible when data is converted from a paper record. However, this does not mean that data acquired in the past is not useful. That acquired since the mid-1980s will often have relatively precise and accurate navigation data allowing integration with other modern datasets with acoustic methods.

Marine sandy deposits vary in terms of composition, size, thickness, horizontal continuity, and admixture with other materials such as biogenic matter, mud, and gravel or rock. According to (de Souza et al., 2015) beach-quality sands have very specific parametric ranges in properties that are acceptable for placement on beaches, it is necessary.

## 2. Acquisition of seismic profiles

The position is determined by an DGPS system and navigation is performed by Hypack and Maxview software that also gives all the offsets for the equipment employed in the survey. Examples of some projects will be described in terms of the project goals and the geophysical equipment selected for each survey and specific geophysical systems according with the scope of work. In Fig 1 is showed a figure of the set of geophysical equipment employed for sand search survey, and Fig 2 showed a figure of the result seabed identification using side scan sonar in punggur sea.

For amplitude side scan sonar image, and in the multi-frequency system, color, becoming a significant properties of the sea floor, the effect of which is a bully needs to be fixed. The main confounding effect is due to absorption of water; geometric spread; shape beam sonar function (combined transmit-receive sonar beam intensity as a function of tilt angle obtained in this sonar reference frame); sonar vehicle roll; form and function of the seabed backscatter (proportion incident on the seabed backscattered signal to sonar as a function of the angle of incidence relative to the sea floor); and the slope of the seabed. Absorption and geometrical spreading effect can be corrected relatively straightforward. The effect of the functions of the sonar beam and seabed functionality angular backscatter which is on the effect of time-varied and more difficult to take into account. It is only relatively recently that sufficient correction has been designed (Tamsett et al., 2016). The seabed backscatters incident sonar signal because: there are acoustic impedance contrasts across the seabed interface; and the seabed interface is rough in comparison to the wavelength of the sonar carrier wave.

The seabed interface comprises usually a seabed surface where one is well defined and shallow sub-seabed surfaces between contrasting materials. High absorption of ultrasound in sub-seabed materials severely limits the skin depth of the interface. The backscatter response of a seabed to the incident sonar signal, being dependent on seabed interface roughness, is therefore dependent on the wavelength of a sonar's carrier wave: i.e., the seabed is acoustically colourful (Buscombe, 2017).

That the seabed is intrinsically acoustically colourful may be recognised in developing a sonar technology and data at multiple sonar frequencies acquired and mapped to optical primary colour frequencies to generate optical colour images of the seabed for human visualization. The principal advantage of colour imagery over greyscale is that at each pixel, a colour datum occupies a position in a three-dimensional (3D) RGB (red, green, blue) data space. If colour data are reduced to greyscale, the data in three dimensions are projected onto and will then occupy positions on a line (e.g., the diagonal across the RGB data space). As econdary advantage of colour sonar images of the seabed is that they can (subject to the eye of the beholder) be very beautiful (Engquist et al., 2017).

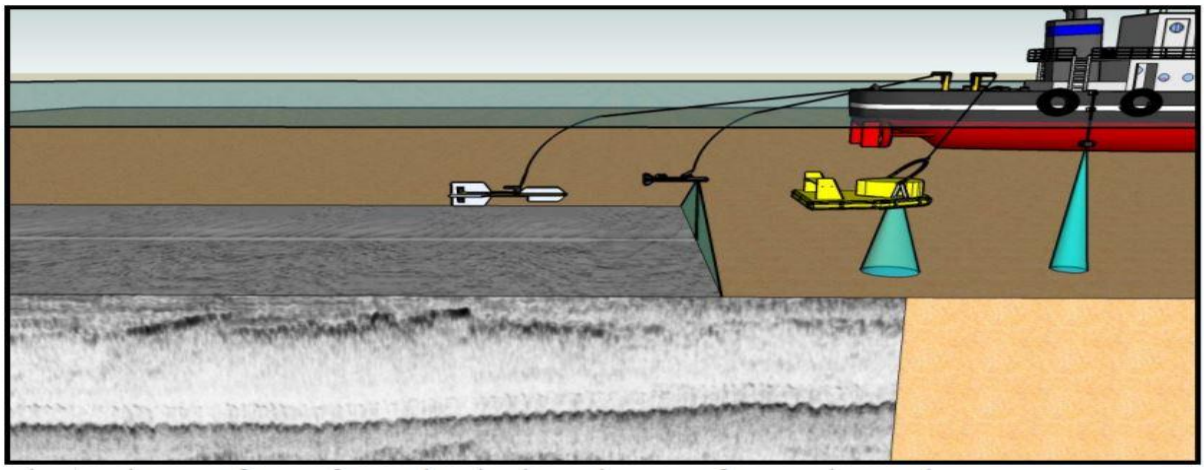

Fig 1. Figure of set of geophysical equipment for sand search surveys (de Souza *et al.*, 2015).

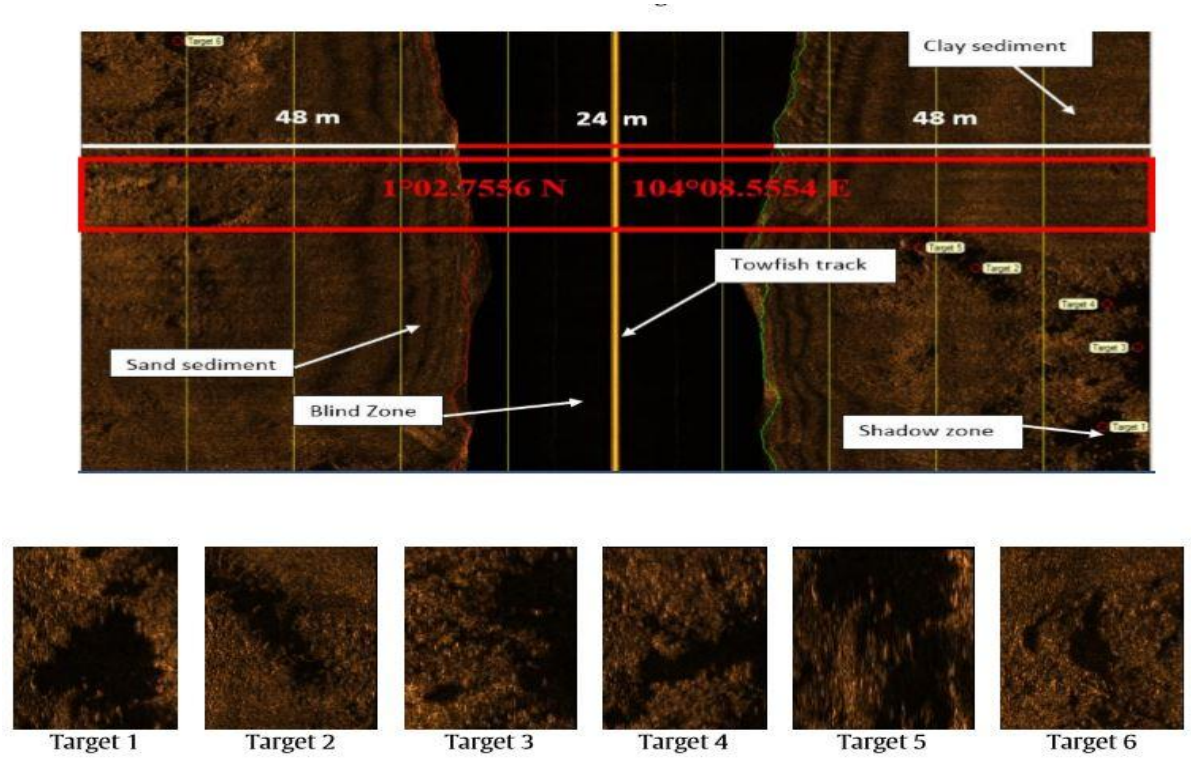


Fig 2. Image classification and position target 1- 6 on sediment track 2, Punggur sea (Lubis et al., 2017).

### 3. Acoustic Colour of the Seabed

Before considering methods for rendering multi-frequency sonar data as colour images,we look a little more deeply at the concept of the acoustic colour of the seabed. Where a sonar system is calibrated, the calibrated backscatter amplitude response of the seabed may be computed from:

$$Scal = \frac{S}{Rcal \,.\, Tcal} \quad (a\ pure\ ratio) \tag{1}$$

where:

- Scal is the calibrated or natural amplitude response of the seabed, this being the ratio of the acoustic signal amplitude backscattered from a seabed to the signal incident on the seabed along the same line (0 to 1.0);
- S is the sonar amplitude response of the seabed (a large integer) corrected for: geometrical spreading incorporating the effect of the area of the seabed ensonified by the sonar pulse, absorption, and the sonar beam function (data along the trace are normalised to the response at the reference inclination angle in the sonar's frame of reference);
- Rcal is the ratio of the amplitude response of the sonar receiver in sonar amplitude units (a large integer) to the pressure amplitude at the receiver in micro-Pascal;
- Tcal is the amplitude of the sonar pulse in micro-Pascal one meter from the transmitter in the direction of the reference inclination angle.

The calibrated amplitude response of the seabed Scal, is afunction of sonar carrier wave frequency ν and angle of incidence with respect to the frame of reference of the seabed (the grazing angle) θ. The function Scal (ν, θ) is two-dimensional and is the broadband seabed backscatter function encapsulating the acoustic backscatter characteristics of a seabed. The dependence on frequency is what makes the seabed acoustically colourful (by definition). The hyper-colour property inherent in Scal (ν, θ) cannot be directly visualised. The generalised function Scal(ν, θ) must be reduced to values at three discrete frequencies (or averaged over three frequency bands) and the values scaled to 8-bit values (zero to 255) for display in pixels in digital visual technologies:

$$nDatR\,(\theta) = 255\,.\,Scal\,(\nu_{low},\,\theta)$$

$$nDatG\,(\theta) = 255\,.\,Scal\,(\nu_{med},\,\theta)$$

$$nDatB\,(\theta) = 255\,.\,Scal\,\left(\nu_{high},\,\theta\right) \tag{2}$$

The values of nDatR (θ), etc., may then be used for computing RGB components of the natural

acoustic colour of the seabed for the frequencies Vlow, Vmed, Vhigh as a function of grazing angle θ, i.e., the values may be used to present the seabed backscatter function measured by a colour sonar system as a line of colour. To display a sonogram montage as a chart, the backscatter values along traces (across sonograms) are normalised to the seabed response at the reference inclination angle θref, say 30″ (Tamset et al., 2016). At angles much less than normal incidence, the natural backscatter amplitudes are small and visually not very distinguishable from shadow. To generate mid-range colours more appropriate for practical human visualisation, an amplitude gain might need to be applied.

$$nDatR = ampGain \,.\, 255 \,.\, Scal\left(v_{low},\, \theta_{ref}\right)$$

$$nDatG = ampGain \,.\, 255 \,.\, Scal\left(v_{med},\, \theta_{ref}\right)$$

$$nDatB = ampGain \,.\, 255 \,.\, Scal\left(v_{high},\, \theta_{ref}\right) \qquad (3)$$

These values may be directly used as parameters for displaying colour for human visualisation or may be used as input to a process for generating other RGB parameters for colour display. Optical colour derived from these values should be specified as having been generated with respect to: the values of the carrier wave frequencies of the system (or the means of bands); the reference inclination angle; and the amplitude gain applied. The relative RGB values are objectively determined by the sonar's calibration data.

An example of a colour sonogram presented in RGB colour is shown in Figure 3.

The values for nDatR, nDatG and nDatB are proportional to the sonar amplitudes as a function of frequency. A value of zero represents shadow and appears as black. A value of 255 represents saturation and appears white. A strongly backscattering seabed appears as light shades of colour, e.g., the light shades of blue running up the right side of Figure 3 bare strongly backscattering. Conversely, aweakly backscattering seabed appears as dark shades of colour; the dark shades of blue running up the left side of Figure 3 are a very weakly backscattering seabed.

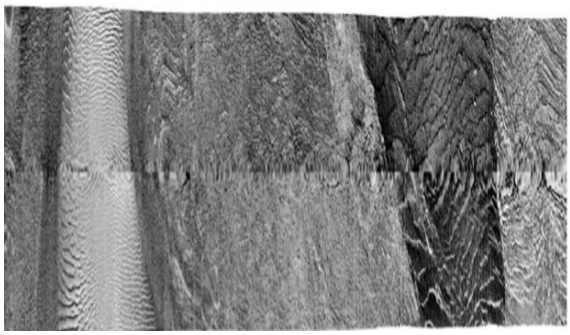

Fig 3. Mid-frequency and componentsofamulti-frequency sonar swath represented as negative greyscale images.

## 4. Angular Bining of The Sonar

The different angles of view are generated by the translation of the sonar. Because of the discrete steps involved by the sequential pings, the angular sampling of the bottom within the ranges described in the previous section is not continuous (Haniotis *et al.,* 2015). We are looking here at the optimal binning of the grazing angles {gi} used to sort the backscatter angular responses, to provide a gapless coverage. The trajectory of the platform is assumed to be a straight line, with the forward step being a constant, Δx, between successive pings. For the sake of clarity, one considers the stop and hop scenario. In addition, the angular sampling is studied in the vertical plane that contains the platform track, the ground profile being horizontal, at depth h below the antenna.

A point of the bottom lying at the abscissa x ahead of the sonar nadir (y = 0) during a ping is viewed under the grazing angle g = π/2 − arctan (x/h). Because Δx ≪ h, the change between successive pings in the angle of view of the same area is approximately $\Delta g \approx (\Delta x/h)\sin^2 g$ (Fig. 4).

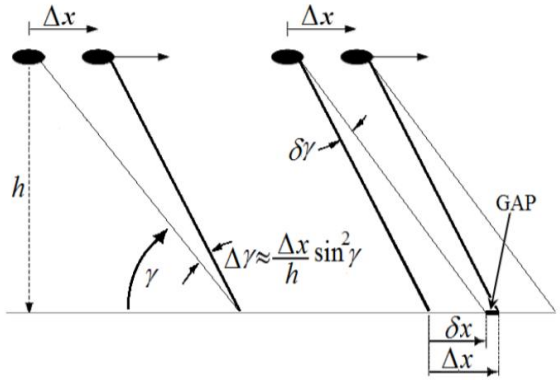


Fig 4. Variation in the angles of view Δg and binning δg (case δg < Δg).

To provide a gapless angular sampling of the bottom, the longitudinal extent δx of the segments intercepted on the bottom by the sectors δγ corresponding to the bin that contains the grazing angle g must be larger than the forward step Δx of the sonar between pings, i.e., there must be δg ≥ Δg. An upper bound of the bin widths is given by the change of view of the nadir area, Δg ≈ Δx/h. With data acquired at sea, the distance Δx is typically a few meters, and the water level, h, is a few tens of meters. Statistics made on the processed surveys yield the order of magnitude Δγ max = 1/12 ≈ 5°. Given an initial grazing angle γ0 (= 69°), the first part of the partition is thus built recursively by considering constant longitudinal footprints, i.e., cotgi+1−cotgi ≈ Δγmax:

$$\gamma_i = \operatorname{arccot}\left(\cot\gamma_0 + i\Delta\gamma_{\max}\right)$$

$$\delta\gamma_{i+1} = \gamma_i - \gamma_{i+1} \approx \Delta\gamma_{\max}\sin^2\frac{\gamma_{i+1}+\gamma_i}{2}. \qquad (4)$$

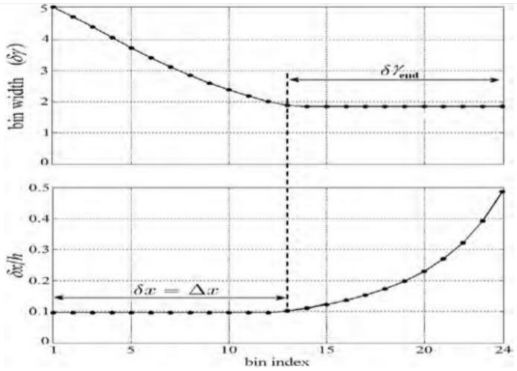

Fig 5. Binning of the grazing angles in the interval [69°, 14°], with Δγmax = 5º and δγend = 2º. (top) Angular bin width δγ. (bottom) Longitudinal extension of the bins.

For low grazing angles, the width of the bins dictated by a constant longitudinal interval $\delta x = \Delta x$ turns out to be very small, which is not justified by the experimental accuracy and increases unnecessarily the number of bins. Consequently, the second part of the partition is built with a constant angular bin width when it reaches a chosen threshold, $\delta\gamma_{end} = 2°$ (Fig. 5). The resulting grazing angles at the limit of the bins are displayed in Fig. 6.

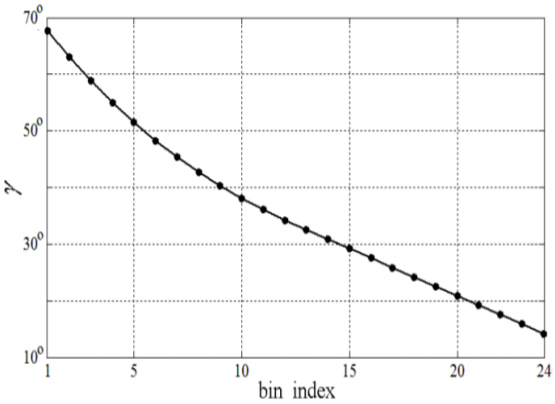

Fig 6. Grazing angles at the limits between bins.

## References


Bartholoma A. 2006. Acoustic bottom detection and seabed classification in the German Bight, Southern North Sea. Springer : Wilhelmshaven, Germany. Vol (26): 177 – 184.

Buscombe, D. 2017. Shallow water benthic imaging and substrate characterization using recreational-grade sidescan-sonar. Environmental Modelling & Software, 89, 1-18.

de Souza, J. A., do Carmo Barletta, R., Franklin, L., & Benedet, L. 2015. Utilization of multiple geophysical sources and geotechnical sampling to search for offshore sand deposits for beach restoration in Brazil. In Acoustics in Underwater Geosciences Symposium (RIO Acoustics), 2015 IEEE/OES (pp. 1-4). IEEE.

Engquist, B., Frederick, C., Huynh, Q., & Zhou, H. 2017. Seafloor identification in sonar imagery via simulations of Helmholtz equations and discrete optimization. Journal of Computational Physics, 338, 477-492.

Haniotis, S., Cervenka, P., Negreira, C., & Marchal, J. 2015. Seafloor segmentation using angular backscatter responses obtained at sea with a forward-looking sonar system. Applied Acoustics, 89, 306-319.

Lubis, M. Z., & Anurogo, W. 2016. Fish stock estimation in Sikka Regency Waters, Indonesia using Single Beam Echosounder (CruzPro fish finder PcFF-80) with hydroacoustic survey method. Aceh Journal of Animal Science, 1(2).

Lubis, M. Z., & Manik, H. M. 2017. Acoustic systems (split beam echo sounder) to determine abundance of fish in marine fisheries. Journal of Geoscience, Engineering, Environment, and Technology, 2(1), 76-83.

Lubis, M. Z., Anurogo, W., Khoirunnisa, H., Irawan, S., Gustin, O., & Roziqin, A. 2017. Using Side-Scan Sonar instrument to Characterize and map of seabed identification target in punggur sea of the Riau Islands, Indonesia. Journal of Geoscience, Engineering, Environment, and Technology, 2(1), 1-8.

Lubis, M. Z., Wulandari, P. D., Mujahid, M., Hargreaves, J., & Pant, V. 2016. Echo Processing and Identifying Surface and Bottom Layer with Simrad Ek/Ey 500. Journal of Biosensors and Bioelectronics, 7(3), 1000212.

Manik, H. M. 2011. Underwater Acoustic Detection and Signal Processing Near the Seabed, in Sonar Systems. Edited by Nikolai Kolev. First Edition. InTech, Croatia. Hal. : 255- 274.

Manik, H. M., Rohman, S., & Hartoyo, D. 2014. Underwater multiple objects detection and tracking using multibeam and side scan sonar. International Journal of Applied Information System, 2(2), 1-4.

Mohammedyasin, S. M., Lippard, S. J., Omosanya, K. O., Johansen, S. E., & Harishidayat, D. 2016. Deep-seated faults and hydrocarbon leakage in the Snøhvit Gas Field, Hammerfest Basin, Southwestern Barents Sea. Marine and Petroleum Geology, 77, 160-178.

Owen, M. J., Maslin, M. A., Day, S. J., & Long, D. 2015. Testing the reliability of paper seismic record to SEGY conversion on the surface and shallow sub-surface geology of the Barra Fan (NE Atlantic Ocean). Marine and Petroleum Geology, 61, 69-81.

Tamsett, D., McIlvenny, J., & Watts, A. 2016. Colour sonar: Multi-frequency sidescan sonar images of the seabed in the Inner Sound of the Pentland Firth, Scotland. Journal of Marine Science and Engineering, 4(1), 26.

Yoo, D. G., Kang, N. K., Bo, Y. Y., Kim, G. Y., Ryu, B. J., Lee, K., & Riedel, M. 2013. Occurrence and seismic characteristics of gas hydrate in the Ulleung Basin, East Sea. Marine and Petroleum Geology, 47, 236-247.